Accurate description of the quantum dynamical surface temperature effects on the dissociative chemisorption of H2 from Cu(111)

Smits, B.; Litjens, L.G.B.; Somers, M.F.

The Journal of Chemical Physics

Accurate description of the quantum dynamical surface temperature effects on the dissociative chemisorption of H_2 from Cu(111)

Cite as: J. Chem. Phys. **156**, 214706 (2022); https://doi.org/10.1063/5.0094985
Submitted: 07 April 2022 • Accepted: 12 May 2022 • Accepted Manuscript Online: 12 May 2022 • Published Online: 02 June 2022

B. Smits, L. G. B. Litjens and M. F. Somers

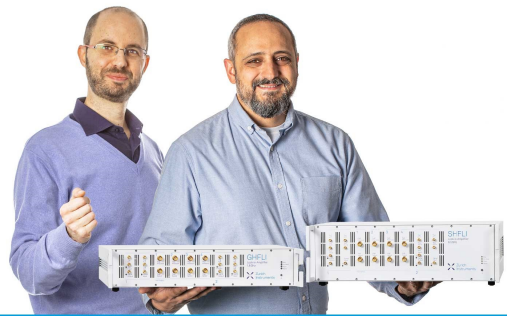

The Journal of Chemical Physics ARTICLE scitation.org/journal/jcp

Accurate description of the quantum dynamical surface temperature effects on the dissociative chemisorption of H_2 from Cu(111)

Cite as: J. Chem. Phys. 156, 214706 (2022); doi: 10.1063/5.0094985
Submitted: 7 April 2022 • Accepted: 12 May 2022 •
Published Online: 2 June 2022

B. Smits, L. G. B. Litjens, and M. F. Somers[a)]

AFFILIATIONS

Leiden Institute of Chemistry, Gorlaeus Laboratories, Leiden University, RA Leiden 2300, The Netherlands

[a)]Author to whom correspondence should be addressed: m.somers@chem.leidenuniv.nl

ABSTRACT

Accurately describing surface temperature effects for the dissociative scattering of H_2 on a metal surface on a quantum dynamical (QD) level is currently one of the open challenges for theoretical surface scientists. We present the first QD simulations of hydrogen dissociating on a Cu(111) surface, which accurately describe all relevant surface temperature effects, using the static corrugation model. The reaction probabilities we obtain show very good agreement with those found using quasi-classical dynamics (QCD), both for individual surface slabs and for an averaged, thus Monte Carlo sampled, set of thermally distorted surface configurations. Rovibrationally elastic scattering probabilities show a much clearer difference between the QCD and QD results, which appears to be traceable back toward thermally distorted surface configurations with very low dissociation probabilities and underlines the importance of investigating more observables than just dissociation. By reducing the number of distorted surface atoms included in the dynamical model, we also show that only including one surface atom, or even three surface atoms, is generally not enough to accurately describe the effects of the surface temperature on dissociation and elastic scattering. These results are a major step forward in accurately describing hydrogen scattering from a thermally excited Cu(111) surface and open up a pathway to better describe reaction and scattering from other relevant crystal facets, such as stepped surfaces, at moderately elevated surface temperatures where quantum effects are expected to play a more important role in the dissociation of H_2 on Cu.

I. INTRODUCTION

One of the major focuses in the field of theoretical heterogeneous catalysis simulations is the accurate description of surface temperature effects on gas–solid reactive scattering.[1–13] These are especially of interest as they form an important basis for many industrial processes, such as the Haber–Bosch process[14] or H_2 powered engines.[15] To obtain the most accurate description, these processes are broken down into their elementary steps, and a focus is put on describing each step individually.

In the past, often one relied on the Born–Oppenheimer static surface (BOSS) approximation, where the surface is assumed to be both fully static and with the atoms in their ideal lattice positions, and electron and nucleus dynamics are assumed to be fully separable.[1] Dynamics is then performed using a 6D potential energy surface (PES) where all H_2 degrees of freedom are included, which is fit to density functional theory (DFT) results using, i.e., the corrugation reducing procedure (CRP).[16] Often, however, these fitting procedures cannot or do not take into account the distorted nature of a thermally excited surface, while the relevant industrial processes, and even experimental studies, are performed at elevated surface temperatures. Several methods have been introduced over the years that do include these thermal surface effects, such as the reactive force-field (RFF) based approach by Busnengo and coworkers,[3,5,17] the reaction path Hamiltonian (RPH) by Jackson and co-workers,[6,7,13] the effective Hartree potential (EfHP) method by Dutta *et al.*,[8] and the static disorder parameter by Kroes *et al.*,[18] as well as both high-dimensional *ab initio* molecular dynamics (AIMD)[9] and a variety of high-dimensional neural network potentials (HD-NNPs).[19–21] HD-NNPs, in particular, are currently an intensively studied method to describing the PES and have been shown to be usable in a wide variety of systems.[22] However, in

our experience, HD-NNPs also often still require dense datasets, as extrapolation beyond the available dataset can yield wildly unexpected results, and careful planning in determining the symmetry functions.[22] In addition, while significant speedups can be achieved using these NNPs compared to AIMD simulations, we find they are generally not computationally fast enough to be used in state-of-the-art quantum dynamics (QD) simulations, nor have any been tested thoroughly yet by also computing accurate rotational and vibrational inelastic scattering or diffraction probabilities compared to experimental data.[23–25] As such, we believe HD-NNPs have not yet achieved the balance between speed and accuracy required for our application.

The system of choice in our line of work is the dissociative chemisorption of H_2 on a (thermally excited) Cu(111) surface, a particularly well studied model system, which would allow for a comparison to a wide range of both theoretical[4,11,12,20,26–30] and experimental[31–36] results. In particular, this system is being experimentally revisited by Alexandrowicz *et al.*, who have recently measured sharply defined state-to-state diffraction probabilities with their molecular interferometry setup.[36–39] Previous experimental work by Kaufmann *et al.* also fully characterized the slow reaction channel of the H_2/Cu(111) system,[35] which has been shown to have a strong temperature and vibrational dependency,[33,34] but has, to our knowledge, not yet been observed in theoretical studies.

Furthermore, using the specific reaction parameter (SRP) approach to DFT, Díaz *et al.* were already able to reproduce experimental molecular beam results to within 1 kcal/mol with the BOSS model.[26] The static corrugation model (SCM) further improved this BOSS model by adding an accurate description of surface temperature effects to quasi-classical dynamics (QCD) of H_2 dissociating on a Cu(111) surface.[10] The addition of a highly accurate embedded atom method (EAM) potential to generate thermally distorted surface slabs finally improved upon previous iterations of the SCM,[12] which relied on random displacements to generate surface slabs.[10,11] The introduction of the EAM potential also allowed for an explicit inclusion of surface motion into QCD using the dynamic corrugation model (DCM).[12] Reaction and scattering probabilities obtained with this EAM-SCM and EAM-DCM showed good agreement with experimental results and clearly demonstrated the validity of the sudden approximation for the H_2 on Cu(111) system.[12]

Thus, the SCM is a prime candidate for introducing all relevant vibrational degrees of freedom into quantum dynamical simulations without also introducing a very large computational cost associated with introducing many more dynamical variables related to the surface atoms. Quantum effects are expected to be especially important for the description of accurate state-resolved scattering probabilities, particularly for stepped surfaces, such as Cu(211).[40] Quantum effects are also expected to be important for an accurate description of (initially) rovibrationally excited H_2 molecules, or when considering lower surface temperatures (T_s). State-resolved scattering, rovibrationally excited molecules and lower surface temperatures are all important for describing industrial applications or reproducing experimental results. Potentials obtained using the SCM have also shown to be smooth enough to allow for an accurate description of both higher rovibrational states as well as state-resolved inelastic scattering probabilities.[10–12] However, the molecular dynamics used to generate surface slabs, as has been done using the EAM potential for T_s = 925 K, is not expected to yield accurate displacements for surface temperatures lower than 300 K.[41]

The EAM-SCM approach is expected to be transferable to H_2 surface reactions on other transition metals for those systems where static surface distortion and thermal surface expansion are the only relevant surface temperature effects. The work required to expand the EAM-SCM to other hydrogen–transition metal systems can be greatly reduced for those systems where accurate (CRP) PESs and EAM potentials are already available, as those can be directly implemented into the framework, requiring only fitting a coupling potential for the system. Systems with an early reaction barrier exhibit a smaller amount of corrugation, which would reduce the difficulty of fitting an accurate coupling potential.[11]

The sudden approximation that lies at the basis of the SCM is expected to work best at a large mass mismatch between the reactant and the surface atom and at shorter interaction times with the surface. However, for those systems where the mass mismatch between H atoms and the transition metal atoms is very large, even the longer surface interaction times could likely be modeled accurately enough with a static surface. While electronic friction due to electron–hole pair excitations is not included in our model, this has been shown to not be too relevant for the H_2/Cu(111) system.[42] However, for other systems, it might have to be included, which is currently only possible at a classical level.[43–45]

In this work, we present the use of the EAM-SCM to include all relevant surface temperature effects of the dissociation and rovibrationally elastic scattering of H_2 on a 925 K Cu(111) surface employing QD instead of QCD for the dynamics. First, we will discuss the effect of constraining the H_2 molecule to a specific (1 × 1) unit cell using QCD. Then, we show a comparison between reaction and elastic scattering probabilities obtained with QD and QCD, both for BOSS and EAM-SCM, and for individual and specifically distorted surface slabs. This allows us to verify if quantum effects, of H_2 and of the surface within a sudden approximation, are important. Finally, we show the effect of only thermally displacing a single or a limited number of surface atoms and its effect on fully describing the surface temperature effects.

II. METHODS

A. Static corrugation model

First introduced by Wijzenbroek and Somers, the SCM is designed to statically include surface temperature effects to correct perfect lattice BOSS dynamics.[10] With this model, the PES obtained for the perfect surface lattice V_{BOSS} is expanded upon by two additional terms: a coupling potential V_{coup}, which describes the additional interaction between displaced surface atoms and the incoming H_2, and a strain potential V_{strain}, which describes the additional potential energy found from the interaction between distorted surface atoms.[10] These three terms put together then give the total potential

$$V_{DFT}(\vec{r}, \vec{q}, \vec{q}^{\,id}) = V_{BOSS}(\vec{r}^{\,id}(\vec{r}), \vec{q}^{\,id}) + V_{coup}(\vec{r}, \vec{q}^{\,id}, \vec{q}) + V_{strain}(\vec{q}^{\,id}, \vec{q}), \quad (1)$$

where $\vec{q}$ describes the positions of all surface atoms, $\vec{q}_{id}$ describes the ideal lattice positions of all surface atoms, and $\vec{r}$ describes the positions of all adsorbed H atoms. $\vec{r}^{\,id}(\vec{r})$ scales the expanded lattice H_2 coordinates $\vec{r}$ along the c.m. vectors U and V to their ideal lattice coordinates in such a way that they correspond to the same relative coordinates on the surface.[10] When treating the distorted surface as static, this expression can be simplified again, as V_{strain} will stay constant and can thus be neglected during dynamics.

Initial work on the SCM focused on obtaining an accurate continuous expression for the H–Cu coupling potential

$$V_{coup}\left(\vec{r},\vec{q}^{\,id},\vec{q}\right)=\sum_{i}^{\vec{r}}\sum_{j}^{\vec{q}}\Big[V_{\text{H-Cu}}(|\vec{r}_i-\vec{q}_j|)-V_{\text{H-Cu}}(|\vec{r}_i^{\,id}(\vec{r})-\vec{q}_j^{\,id}|)\Big], \tag{2}$$

where $\vec{r}_i$ describes the positions of adsorbate i and $\vec{q}_j$ describes the surface atom position j. This was achieved using a switched Rydberg-like function fit to raw DFT data obtained using the same functional as the BOSS CRP potential[10]

$$V_{\text{H-Cu}}(R)=(1-\rho(R))V(R)+\rho(R)V(P_7), \tag{3}$$

with

$$V(R)=-e^{-P_4(R-P_5)}\left(\sum_{k=0}^{3}P_k(R-P_5)^k\right) \tag{4}$$

and

$$\rho(R)=\begin{cases}0, & \text{for } R<P_6,\\ \frac{1}{2}\cos\left(\frac{\pi(R-P_7)}{P_7-P_6}\right)+\frac{1}{2}, & \text{for } P_6\le R\le P_7,\\ 1, & \text{for } R>P_7.\end{cases} \tag{5}$$

The V_{strain} term of Eq. (1) was not used in the subsequent dynamics due to the static surface approximation. Furthermore, thermal lattice expansion corrections to the BOSS PES component of Eq. (1) were introduced by stretching or contracting the H_2 center of mass (c.m.) vectors along the lattice vectors U and V.[10] A significant improvement to the quality of V_{coup} was made by Spiering *et al.*[11] using an effective three-body potential by linearly scaling the fitting parameters to the H–H bond distance

$$P_i=\begin{cases}P_{i,a}r_{\text{H-H}}^{\min}+P_{i,b}, & \text{for } r_{\text{H-H}}<r_{\text{H-H}}^{\min},\\ P_{i,a}r_{\text{H-H}}+P_{i,b}, & \text{for } r_{\text{H-H}}^{\min}\le r_{\text{H-H}}\le r_{\text{H-H}}^{\max},\\ P_{i,a}r_{\text{H-H}}^{\max}+P_{i,b}, & \text{for } r_{\text{H-H}}>r_{\text{H-H}}^{\max}.\end{cases} \tag{6}$$

Finally, Smits and Somers introduced a very accurate EAM potential for Cu to generate accurate surface slab configurations using molecular dynamics.[12] In contrast, in the previous studies on SCM,[10,11] one relied upon the use of temperature-dependent random surface atom displacements based on experimental neutron scattering data.[46] Furthermore, this EAM potential was used to describe V_{strain}, which enabled the inclusion of a moving surface into what was referred to as the DCM.[12] This allowed for a rigorous test to validate the underlying sudden approach of SCM using QCD and confirmed that reaction, and rotational and vibrational (in)elastic scattering probabilities are not affected by excluding energy exchange between H_2 and the copper surface.[12]

Clearly, the different components of V_{DFT} of Eq. (1) could be implemented using other methods of representing a PES, as explained in the Introduction. We have opted for using the CRP method for the BOSS component, the SCM H–Cu effective three-body pair potential for V_{coup} and a well known and accurate EAM potential for V_{strain}. These specific choices have the following advantages: the CRP method has been extensively used for BOSS calculations in the past, allowing direct comparisons to the EfHP work of Dutta *et al.*,[8] all based on the chemical accurate SRP48 DFT functional and has proven to be fast and accurate enough to even allow for obtaining diffraction probabilities on a QD level.[1,47] The V_{coup} H–Cu potential has also been based on the same SRP48 DFT functional, has been used in the EfHP work of Spiering *et al.*, has been shown to fit within the chemical accuracy,[11] and was determined to be fast enough to be used in QD too.[8] The V_{strain} EAM potential has not been based on the SRP48 DFT functional as this functional was only proven to be of chemical accuracy for the H_2–Cu interactions and most likely is not suitable for describing bulk Cu.[26,27] The EAM, on the other hand, is very accurate in describing the Cu system, both bulk and surface, itself.[41] Moreover, in this new QD-EAM-SCM work, the EAM is only used to obtain surface slabs and to get as realistically correct Cu thermal expansion and atom displacements as possible from MD simulations. In addition, in the previous DCM work of Smits *et al.*, it was found not needed to adjust, fine-tune, or refit the obtained H–Cu V_{coup} potential parameters P_n to correct for the usage of the EAM as V_{strain}.[12] The most important advantage is that, when doing QD, and thus when evaluating V_{DFT} for 10^9 points per time-dependent wave packet (TDWP) run, the expressions used offer a decent balance between accuracy and speed making this work possible and allowing us to compare to previous results investigating the effects of the different components on the dynamical model itself.

B. Quantum dynamics

To perform our 6D QD simulations, we use the TDWP approach to solve the time-dependent Schrödinger equation as follows:

$$i\hbar\frac{d\Psi(\vec{Q};t)}{dt}=\hat{H}(\vec{Q})\Psi(\vec{Q};t), \tag{7}$$

using the split operator method as implemented in our in-house code.[48] Here, $\vec{Q}(X,Y,Z,r,\theta,\phi)$ is the six-dimensional position vector of the H_2, $\Psi(\vec{Q};t)$ the time-dependent nuclear wave function of the system, and $\hat{H}(\vec{Q})$ the time-independent Hamiltonian of the system, described as

$$\hat{H}(\vec{Q})=-\frac{\hbar^2}{2M}\nabla^2-\frac{\hbar^2}{2\,\mu r^2}\frac{\partial^2}{\partial r^2}+\frac{1}{2\,\mu r^2}\hat{J}^2(\theta,\phi)+V(\vec{Q}), \tag{8}$$

with M and μ, respectively, the mass and reduced mass of the hydrogen molecule, and ∇ and $\hat{J}$ the nabla and angular momentum operators.

The 6D PES $[V(\vec{Q})]$ related to each different surface configuration is constructed with the SCM approach as described in Eq. (1), with V_{BOSS} described using the SRP48 CRP PES[9] and V_{coup} described using the effective three-body SCM coupling potential also based on the same SRP48 DFT functional,[11] which has been shown to achieve chemical accuracy.[26] Surface slab configurations are obtained from classical dynamics using the EAM potential, as is described in Ref. 12. V_{strain} can again be ignored in this QD-EAM-SCM work, as the surface is treated on a sudden approximation level during the QD of H_2.

The initial wave function $\Psi(\vec{Q},\ t=0)$ is represented as the product of a Gaussian wave packet $[u(Z;Z_0,k_0^Z)]$ centered around a point far away from the surface, a rovibrational wave function $[\psi_{v,j,m_j}(r,\theta,\phi)]$ of the H_2 and a two-dimensional plane wave function $[\phi(k_0^X,k_0^Y)]$ along X and Y,[40]

$$\Psi(\vec{Q},\ t=0) = \psi_{v,j,m_j}(r,\theta,\phi)\phi(k_0^X,k_0^Y)u(Z;Z_0,k_0^Z), \tag{9}$$

with

$$\phi(k_0^X,k_0^Y) = \exp(i(k_0^X X_0 + k_0^Y Y_0)) \tag{10}$$

and

$$u(Z;Z_0,k_0^Z) = \left(\frac{2\sigma^2}{\pi}\right)^{\frac{1}{4}} \int_0^\infty \mathrm{d}k_0^Z \exp(-\sigma^2(\vec{k}-k_0^Z)) \times \exp(i(\vec{k}-k_0^Z)Z_0) \times \exp(ik_0^Z Z_0). \tag{11}$$

Here, σ is the width of the wave packet centered around the wave vector $\vec{k}$ and $k_0^{X,Y,Z}$ the initial wave vectors of the H_2 c.m.

A quadratic form of the optical potentials in the scattering and adsorption regions is used,[49] while the scattered fraction is analyzed through the scattering matrix formalism,[50] which yields the scattering probability. The sticking probability is subsequently calculated from this scattering probability. In contrast to the more often used flux methods,[21,51] the scattering amplitude method we employ also allows us to extract diffraction probabilities and rovibrationally resolved scattering results. Rovibrationally resolved scattering and diffraction probabilities, in particular, are expected to show a larger quantum dynamical effect compared to the non-quantized quasi-classical results and are thus an important part of this work. For a more in-depth discussion of the basis of these quantum mechanical methods, we direct the reader to Refs. 40, 48, and 52.

We obtain reaction and elastic scattering probabilities using QD for a total of 104 thermally distorted surface slabs, each acquired from a unique trace of molecular dynamics using the EAM potential. The reaction and scattering probabilities are then averaged to get a single representative dissociation or elastic scattering probability curve of H_2 dissociating on, or scattering from, a thermally excited Cu(111) surface. Through the averaging over many thermally displaced surface configurations, the quantum dynamics of the surface atom degrees of freedom is effectively done on a sudden approximation level using Monte Carlo sampling. This essentially means that even for the surface degrees of freedom, we implicitly perform QD, but with the approximation that energy exchange between H_2 and the surface is not possible. Previous work has shown that this approximation holds very well for D_2 on Cu(111), which has a smaller mass mismatch between the surface atoms and the dissociating molecule.[12] There is also no energy exchange possible between the vibrations within the solid during the individual QD TDWP runs, making sure that any classical redistribution or leaking of zero point energy is not possible at all. This is where we think the SCM shines.

For each individual surface configuration, the QD reaction or elastic scattering curve is obtained via three different wave packets, one with an energy range from 0.10 to 0.30 eV, another from 0.25 to 0.70 eV, and a third from 0.65 to 1.00 eV. Details regarding the computational parameters for each of these wave packets are described in the supplementary material.

C. Quasi-classical dynamics

These QD simulations fully including all relevant surface temperature effects are compared to QCD calculations. The QCD calculations on H_2 have been performed similarly to the work published previously for D_2.[12] In contrast to fully classical dynamics, QCD also includes the presence of zero point energy of the initial rovibrational states, which has been shown to be important for describing a H_2 on metal system.[48] The initial rovibrational energy for our specific PES is calculated using the Fourier grid Hamiltonian method,[53] followed by a constant time step propagation for one full vibrational phase to obtain the quasi-classical distribution of the H–H distance. The adsorbate c.m. is always placed 7 Å above the surface in the Z direction. The molecular angles θ and ϕ are randomly chosen from a uniform distribution on the sphere with $\cos(\theta)$ from −1 to 1 and ϕ from 0 to 2π, respectively, while the initial adsorbate c.m. coordinates $U(=X-Y/\sqrt{3})$ and $V(=2Y/\sqrt{3})$ are chosen randomly from a uniform distribution between 0 and a, with a being the lattice constant of the surface slab. Internal angular velocities are chosen according to the quantized angular momentum $L^2 = J(J+1)\hbar^2$, while the angle θ_L between the angular momentum vector and the surface normal is chosen randomly but constrained by $\theta_L = \pi$ for $J = 0$ and $\cos(\theta_L) = m_j/\sqrt{J(J+1)}$ if $J \neq 0$. For a schematic overview of our coordinate system, we refer to Fig. 1.

Surface atom displacements for the EAM-SCM approach are randomly selected from a total of 25 000 surface configurations, obtained from 1000 different traces with molecular dynamics for a modeled surface temperature of 925 K using the EAM potential.[41] Currently, 104 of otherwise exactly the same surface configurations (but randomly selected) used in QCD-EAM-SCM have been used for the QD-EAM-SCM. Only those surface atoms within 16 bohrs of the unit cell corner $(U,V,Z) = (0,0,0)$ and within the top two layers of the distorted surface slab were included for the calculation of the SCM potential, as was done in previous work.[12]

The quasi-classical trajectories are propagated using the simple Hamiltonian

$$H = \sum_{i=0}^{n}\left[\frac{p_i^2}{2m_i}\right] + V(R(t)) \tag{12}$$

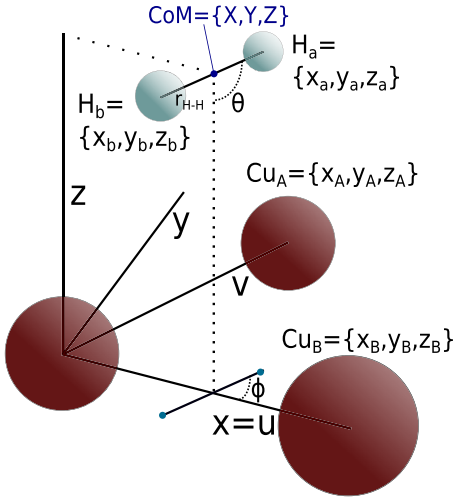

FIG. 1. Coordinate system of our incoming H_2 (light blue) with lattice vectors for the Cu(111) surface slab (dark red). The six DoFs of the incoming H_2 molecule are described both in atomic coordinates (x_a/x_b, y_a/y_b, z_a/z_b) and molecular, center of mass (c.m.) coordinates (X, Y, Z or U, V, Z), with the H–H distance r_{H-H}, the polar angle θ, and the azimuthal angle ϕ relative to the x axis. The surface atoms are described using only atomic coordinates (x_l, y_l, z_l). Reproduced from B. Smits and M. F. Somers, J. Chem. Phys. **154**, 074710 (2021) with the permission of AIP Publishing.

according to Hamilton's equations of motion. Here, p_i and m_i are, respectively, the momentum and mass of the ith atom and $V(R(t))$ describes the total potential energy of all n atoms at positions R and time t. Propagation is performed using the Bulirsch–Stoer predictor–corrector algorithm,[54] ending when the two H atoms move more than 2.25 Å apart for a reactive trajectory, or when the Z c.m. coordinate is further than 7 Å from the surface for a scattered trajectory. For each incidence energy, a total of 50 000 trajectories were performed, each using a unique surface configuration in the QCD-EAM-SCM. Additionally, each of the 104 surface configurations used in QD-EAM-SCM were also separately investigated with 50 000 trajectories per incidence energy using QCD-EAM-SCM. For more in-depth information, we refer to Ref. 12 where the same procedure was used for D_2.

In this work, we also investigate the effect of applying a minimum image convention to the c.m. of the incoming H_2 molecule. When the c.m. moves further outside of the boundaries of 0 to a in both the lattice U and V coordinates, it is mapped back into the (1 × 1) unit cell when computing the PES and/or the forces associated with it. This then makes the actual PES used in the dynamics to be translation symmetric when the molecule leaves the (1 × 1) unit cell. This translation symmetry constraint on the dynamics of H_2 is investigated in detail in order to verify the use of a single (1 × 1) unit cell in the QD. The SCM corrugation V_{coup} interaction could be influenced by such a symmetry constraint, as it is only diminished beyond ~10 bohrs [see the $P7$ parameter of Eq. (5)].[11] The use of a single (1 × 1) unit cell reduces the computational demands for the QD enormously as with the current approach to Monte Carlo sampling over at least 100 individual surfaces, these QD calculations we present here entail a computational challenging task even when using the (1 × 1) single unit cell approximation.

D. Limited atom static corrugation model

In previous studies, models to include surface atom degrees of freedom often focused primarily on distorting one, or a few, of the DoF of the surface atom closest to the reactant impact site.[6,7,29,30,55] To investigate the quality of such an assumption for our system, we aim to also investigate the effect of only including a small number of surface atoms on the reaction and elastic scattering probabilities obtained using the EAM-SCM. Instead of using all atoms found within the 16 bohrs SCM cutoff radius described earlier in this section, distorted surface atoms are ranked based on their distance from the middle of the top layer of the (1 × 1) unit cell $[(U,V,Z) = (\frac{a}{2}, \frac{a}{2}, 0)]$ and only a limited number are now included in the model. All other surface atoms are kept at their ideal lattice positions. This procedure allows us to easily navigate the approximations one makes if including only a limited number of surface DoFs at both the QCD as well as the QD level of theory. This method we will refer to as the limited atom SCM, or NAt-EAM-SCM. Here, N stands for the number of surface atoms included, in this work 1At, 3At, and 5At, for one, three, and five surface atoms, respectively.

III. RESULTS AND DISCUSSION

By comparing the results from QD and QCD simulations of the dissociative chemisorption of H_2 on Cu(111), we aim to verify the quality of the SCM approach to including surface temperature effects into the QD simulations of the hydrogen molecule. Our focus will be on the rovibrational ground state of H_2. In particular, we compare the results obtained using the QD-EAM-SCM to QCD-EAM-SCM. The QD-EAM-SCM implements the QD of H_2 directly and fully correlated, but, as stated before, the QD of the surface atom degrees of freedom are treated on a sudden approximation level using Monte Carlo sampling. The QCD-EAM-SCM uses QCD for the dynamics of H_2 but again treats the dynamics of the surface on the same sudden approximation level, but with many more unique surface samples included compared to QD-EAM-SCM. The QCD-EAM-SCM has been previously validated for D_2, to the dynamic corrugation method (DCM), where the surface was allowed to move.[12] It was found that the energy exchange possible in the DCM, but not in the SCM, was negligible (for D_2, which as a higher mass than H_2). We are, therefore, confident that the sudden approximation of the SCM for H_2 will hold even better and allow us to perform the QD-EAM-SCM, via Monte Carlo sampling, on such a scale.

The surface configurations we use in this EAM-SCM approach, both for the QCD and QD, were obtained from classical dynamics using the EAM potential at a modeled surface temperature of 925 K. This surface temperature was chosen to be able to compare to the experimental results,[28,32] but is also well within the classical regime for this Cu system. This implies the correct use of the Maxwell–Boltzmann statistics, inherent to molecular dynamics, in the effective Monte Carlo sampling in both QCD-EAM-SCM and QD-EAM-SCM.

A. Constrained results

One of the main constraints of our QD implementation is the size of the unit cell that can feasibly be used in the TDWP method. Moving from a (1 × 1) to a (2 × 2) unit cell would already increase computational costs by a factor of four. While a small unit cell can easily be used with the BOSS approach, due to the periodicity of the ideal surface lattice, the same cannot be assumed when thermally distorting the lattice. Therefore, we first investigated the effect of constraining the H_2 molecule to a (1 × 1) unit cell of the surface using, computationally much cheaper, QCD simulations. This translation symmetry constraint was simply implemented by always mapping the H_2 c.m. U and V coordinates into the single (1 × 1) unit cell before calculating the actual PES and the forces derived from it.

In Fig. 2, we show the reaction and elastic scattering probabilities obtained with QCD for the H_2 on a Cu(111) surface at a modeled surface temperature of 925 K, both for the (1 × 1) unit cell constrained (1 × 1)-EAM-SCM and for the unconstrained EAM-SCM. Included are the rovibrational ground state (a, v,J = 0,0) as well as vibrationally (b, v,J = 1,0), rotationally (c, v,J = 0,11), and rovibrationally (d, v,J = 1,11) excited initial states. Agreement between the constrained and non-constrained EAM-SCM results seems perfect for all four rovibrational states included, both for the reaction and elastic scattering probabilities. This excellent agreement confirms that the SCM does still yield accurate results when the H_2 molecule is constrained within a (1 × 1) unit cell of the surface for QCD and likely also for QD.

B. Dissociative chemisorption and rovibrationally elastic scattering

With confirmation that the SCM still yields accurate results for H_2 constrained to a small (1 × 1) unit cell, we next include the EAM-SCM into our QD calculations. In Fig. 3, we display the reaction (a) and rovibrationally elastic scattering (b) probability curves for the QD-EAM-SCM model, obtained as an average of calculations on 104 unique EAM generated surface slabs at a modeled surface temperature of 925 K. We also include the QCD-EAM-SCM results both as an average of the 104 surface slabs used in the QD-EAM-SCM calculations and from a random selection out of the 25 000 surface slabs available, as was done in previous work.[12] This allows us to get an estimate on the error we can expect when only including such a relatively low number of unique surface slabs into our QD-EAM-SCM model. Furthermore, we also compare our results to those obtained by Dutta *et al.*, who applied their EfHP method to include thermal surface displacements into QD simulations for the same H_2/Cu(111) system, using the same underlying BOSS CRP PES and SCM V_{coup} potentials, all based on the same SRP48 DFT functional, and using exactly the same TDWP code.[8] Finally, we also include the results obtained using the perfect lattice BOSS approach both with QD and QCD, as has often been investigated in the past.

As expected, each dissociation probability curve shows a slow buildup at low incidence energy as most incoming adsorbates do not have enough energy to pass over the reaction barrier. At higher incidence energies, we find a mostly linear relation between the incidence energy and reaction, which will then eventually level off to a saturation value at energies well out of the plotted range. Only the QD-BOSS results show a slight deviation in this analysis, with a small "bump" in reaction probability around a normal incidence energy of 0.7 eV. The EfHP results display by far the lowest reactivity, which can be explained by this model only including thermal displacements and not lattice expansion, as well as making other approximations related to the effective Hartree approach.[8,10] Agreement between the reaction probabilities obtained for the

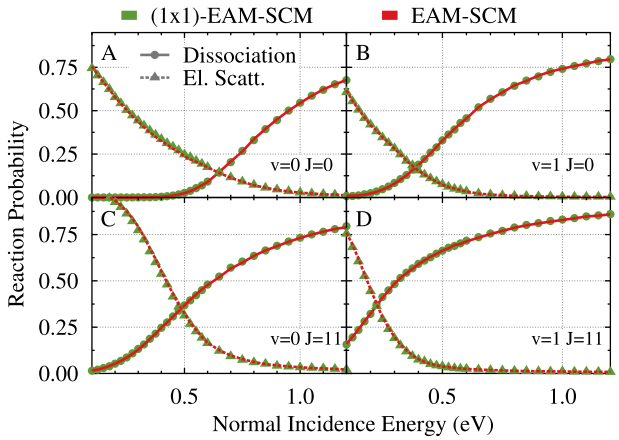

FIG. 2. Reaction and rovibrationally elastic scattering probabilities obtained using both the (1 × 1)-EAM-SCM (green circles) and regular EAM-SCM (red curves). Reaction is shown as solid circles and lines, while the elastic scattering is shown as triangles and dashed lines. Included are: (a) the rovibrational ground state v = 0, J = 0; (b) a vibrationally excited state v = 1, J = 0; (c) a rotationally excited state v = 0, J = 11; (d) a rovibrationally excited state v = 1, J = 11. The system of choice is H_2 reacting on a thermally distorted Cu(111) surface at a modeled surface temperature of 925 K.

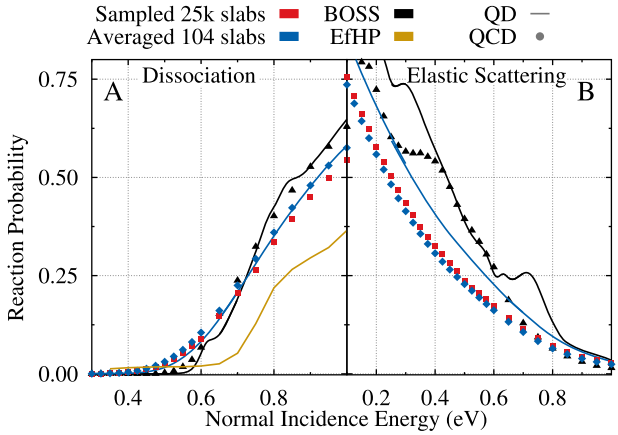

FIG. 3. Reaction (a) and rovibrationally elastic scattering (b) probability curves for the H_2 in the rovibrational ground state (v = 0, J = 0) on a Cu(111) surface. Included are the results obtained using the EAM-SCM both for a random sampling over all 25 000 surface slabs with QCD (red squares) and an average of 104 selected surface slabs using both QD (blue curve) and QCD (blue diamonds). BOSS results for QD and QCD are shown as a black curve and black triangles, respectively. Finally, reaction probabilities from other work by Dutta *et al.*, obtained using the QD EfHP approach,[8] are shown as a yellow curve. For the EAM-SCM and EfHP results, a modeled surface temperature of 925 K is used.

104 surface slabs compared to the results for a random selection of 25 000 surface slabs for QCD-EAM-SCM is good, which implies only a small error is expected in our QD-EAM-SCM results due to the relatively few surface slabs used. However, some small variation is observed, indicating better results could be obtained if the number of included surface slabs is increased. Clearly, this is possible at the expense of using more computational resources by simply running more TDWP QD runs. We have chosen, in view of the limited time, for using ≈100 surfaces for the QD-EAM-SCM and by estimating the error by simply comparing to QCD-EAM-SCM results.

Interestingly, both the QCD-EAM-SCM and QD-EAM-SCM results show a much earlier curve onset, while also not increasing as steeply toward their maximum value. This broadening of the reaction probability curve is generally associated with surface temperature effects, as has been seen in previous work.[10,28,56] Furthermore, the agreement between the QCD-EAM-SCM and QD-EAM-SCM results is also very good, with the QD curve displaying slightly less broadening. This is a strong indication of an accurate description of thermal surface effects in our QD results. However, this agreement is not perfect and thus also demonstrates subtle quantum effects do already come into play for the reaction of hydrogen on a 925 K copper surface.

When we consider the elastic scattering in Fig. 3(b), we observe much less subtle quantum effects. Again, the agreement between the scattering probabilities obtained for the 104 surface slabs compared to the results for a random selection of 25 000 surface slabs for QCD-EAM-SCM is good. The BOSS results show some variation between QCD and QD, although this can be mostly attributed to the "bumps" we see around 0.3 and 0.7 eV, which have been reported in previous studies using this SRP48 PES.[12] However, a clear difference is now visible when comparing the QD-EAM-SCM and QCD-EAM-SCM results, where QD shows a much higher probability for elastic scattering at lower incidence energies. This observation underlines the importance of properly investigating a system using QD and shows the limited information available when only reaction probabilities are investigated and compared. Furthermore, these quantum effects could become even more important for higher initial rovibrational states of the H_2, for rovibrational inelastic scattering and/or diffraction. It is expected to be especially important for lower surface temperatures or scattering reactions from stepped surfaces [Cu(211)], but at the present time this has not been investigated thoroughly yet, partly due to the computational challenges associated with these systems. However the SCM approach, for H_2 and D_2, and the use of the scattering amplitude formalism in the QD really shine here.

To further investigate the quality of the QD dynamics compared to our QCD results, we take a closer look at the reaction and elastic scattering results on a few individual thermally distorted surface slabs. Especially of interest are those surfaces where the dissociation probability is either much higher or lower than on average. This allows us to validate the model not just on average when Monte Carlo sampling over many surface configurations, but also for the specific edge cases it will have to deal with.

In Fig. 4(a), we show reaction probabilities for three different surface slabs: not very reactive (surface α), very reactive (surface β), and typical (surface γ). Also included are the averaged results for all the EAM-SCM distorted surface slabs.

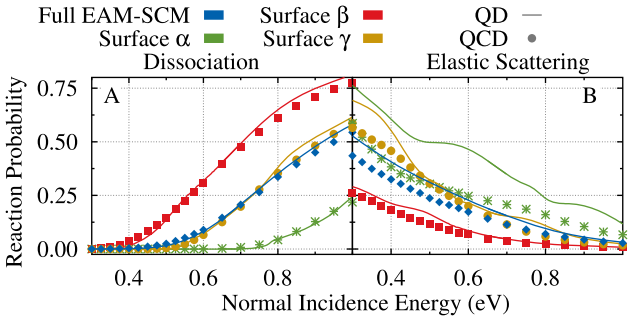

FIG. 4. Reaction (a) and rovibrationally elastic scattering (b) probabilities for three specific thermally excited surface slabs, and the average of all investigated distorted surface slabs, all for a modeled surface temperature of 925 K with the incident H_2 in the rovibrational ground state. Results for surface α, β, and γ are shown as green stars and lines, red squares and lines, and yellow circles and lines, respectively, while the results for the averaged probabilities obtained using the EAM-SCM are shown as blue lines and diamonds. Here, the lines represent the QD results, while the symbols represent the QCD results. For the full EAM-SCM results, the QD curves consist of an average of 104 surface slabs, while the QCD results are obtained from random sampling of all 25 000 distorted surface slabs.

For dissociation, we again see the characteristic S-curve shape, with the results for the more reactive surface slab β already leveling off toward a saturation value. In contrast, the curve of the non-reactive surface slab α just passed the curve onset and is reaching the linear part of the S-curve. Overall, the agreement between the QCD results as symbols and the QD results as a line is excellent. As was the case for the Monte Carlo sampled results, we see a small decrease in curve broadness for QD compared to QCD, which is more visible for the results of slab β than for the other two.

In general, we see no great variation in the agreement between QCD and QD when we compare the reaction probabilities found for the individual surface slabs to those obtained for the general average. However, no such claim can be made for the elastic scattering probabilities, as can be seen in Fig. 4(b). We find great agreement between the rovibrationally elastic scattering probabilities obtained using the reactive surface slab β, while the agreement between the QD and QCD probabilities found for the typical slab γ is close in line to that found for the full average of all surface slabs. Furthermore, the probabilities found for the non-reactive surface slab α show the largest difference between the QD- and QCD-EAM-SCM. This appears to indicate that the differences between the QD and QCD elastic scattering probabilities we find in Fig. 3(b) are primarily caused by those surface slabs that have a much higher barrier due to the thermal distortion of the surface. However, much work, also including more surface slabs into the QD-EAM-SCM, will be required to fully understand this phenomenon.

C. Limited surface atom degrees of freedom

In previous studies, the effects of including surface atom degrees of freedom were often described through the displacement of a single surface atom, or even a single DoF of a single surface atom.[6,7,29] While such an approach is computationally very efficient,

it is not too clear if all thermal surface effects can be described through such a small number of degrees of freedom, or even a single one. Using the EAM-SCM, we are able to selectively include, or exclude, the contribution of specific distorted surface atoms. With this, we aim to investigate the effect of reducing the number of surface atoms taken into account for the thermal surface effects of the H_2 on Cu(111) system, both in QD and QCD.

In Fig. 5, we show the reaction and rovibrationally elastic scattering probabilities obtained with QD- and QCD-EAM-SCM when only including one, three, or five thermally distorted Cu(111) surface atoms. The surface atoms to include were selected based on their distance from the center of the (1 × 1) Cu(111) surface unit cell, starting with the closest. Also included are the results of the full EAM-SCM model, which includes ~70 surface atoms depending on the specific distorted surface slab used, and the BOSS results.

Again, agreement between reaction probabilities obtained with QD-EAM-SCM and QCD-EAM-SCM appears to be very good, even for those results where less surface atoms are included in the model. Similarly, we see a clear decrease in elastic scattering probabilities obtained with QD-EAM-SCM compared to QCD-EAM-SCM for all the EAM-SCM results. However, there is also a clear difference between the EAM-SCM results where less surface atoms are taken into account, both for reaction and scattering probabilities. In particular, the results obtained when only a single surface atom is thermally displaced show much more "BOSS-like" probabilities, with less of the broadening usually attributed to surface temperature effects. Adding two more surface atoms to the model already greatly increases agreement with the full EAM-SCM model, although there is still a noticeable discrepancy with the results obtained with the full model. Finally, the 5At-EAM-SCM results show excellent agreement with the full model, which appears to indicate that correctly implementing surface temperature effects will require at least five surface atoms to be included to get accurate results for the H_2 on Cu(111) system when including a modeled surface temperature of 925 K. That using only five surface atoms already gives such good results correlates with the effectiveness of only using a single (1 × 1) unit cell for the QD, as only ~10 surface atoms are found within the ≈7 bohrs distance where V_{coup} contributes significantly toward the potential energy of the PES.[11] This is an important characteristic to keep in mind when designing new models for including the surface temperature, although it is currently unclear if this characteristic is specific for our system, or even the model used to describe it.

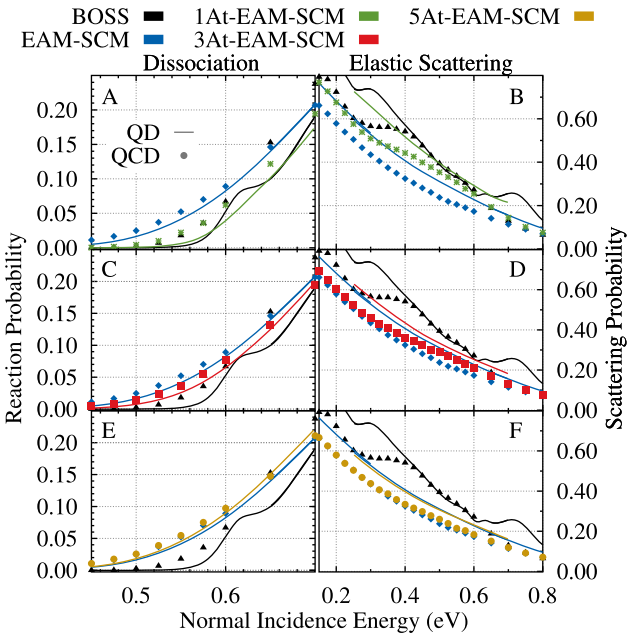

FIG. 5. Reaction [(a), (c), and (e)] and rovibrationally elastic scattering [(b), (d), and (f)] probabilities obtained for the 1At-, 3At-, and 5At-EAM-SCM approach, as well as the full EAM-SCM and BOSS approaches. Here, 1At, 3At, and 5At refer to the number of surface atoms included into the EAM-SCM and are shown as green stars and lines [(a) and (b)], as red squares and lines [(c) and (d)], and as yellow circles and lines [(e) and (f)], respectively. The BOSS results are included as black lines and triangles, and the full surface EAM-SCM results are shown as blue diamonds and lines. The lines represent the QD results, while the symbols represent the QCD results. For the EAM-SCM results with one, three, five, and all thermally distorted surface atoms (within the cutoff) included, the QD curves consist of an average of 104 surface slabs, while the QCD results are obtained from random sampling of all 25 000 distorted surface slabs.

IV. CONCLUSION

We investigated the quality of the EAM-SCM in quantum dynamical calculations to accurately describe all relevant surface temperature effects. Dissociation and rovibrationally elastic scattering probabilities were computed, using both QCD and QD, for the H_2 on Cu(111) system at a modeled surface temperature of 925 K for the rovibrational ground state. Similar to previous studies, a CRP PES based on the SRP48 functional was used, which has been shown to be chemically accurate.[26] The SCM coupling potential was described using the effective three-body potential as published by Spiering *et al.*,[11] while the surface configurations used were published by Smits and Somers[12] and obtained with molecular dynamics using a highly accurate EAM potential.[41]

Before implementing the SCM into our QD calculations, we first investigated the effect of constraining the H_2 molecule to a (1 × 1) unit cell, as much larger cells are computationally unfeasible for QD. Reaction and elastic scattering probabilities obtained using QCD and a variety of rovibrational states showed excellent agreement between those simulations where the H_2 molecules were and were not constrained.

With confirmation that the SCM would yield accurate results, even when such a small unit cell is used, we next included the EAM-SCM into our quantum dynamics. Both the QCD and QD reaction probability curves obtained using the SCM showed the characteristic curve broadening compared to the BOSS results found when surface temperature effects are taken into account. Furthermore, the QCD- and QD-EAM-SCM results showed great agreement with each other when considering the reaction probability, which indicates the quality of the quasi-classical approach for this system and observable. The QD-EAM-SCM results did display a very slight decrease in curve broadening, which clearly indicates a quantum effect that could be of importance. For the elastic scattering, however, even more differences were found. Instead, the

QD elastic scattering probabilities were found to be significantly higher than the QCD results, which could indicate an important quantum effect for this system. For the BOSS model, the difference in the scattering probability was much less apparent, which could indicate a role of surface temperature effects or our model in particular.

To further investigate this difference between QD and QCD, we next compared reaction and scattering probabilities obtained for several specific distorted surfaces using the EAM-SCM. A highly reactive, highly non-reactive, and a typical surface slab were chosen for comparison to get an overview of the different types of surface slabs available. Again, reaction probabilities were found to have great agreement between QD and QCD, even for the three specific surface slabs, although the highly reactive slab again displayed a small difference in curve broadness between QD-EAM-SCM and QCD-EAM-SCM. Interestingly, elastic scattering probabilities obtained for the typical and highly reactive surface configurations also showed great agreement between the QCD and QD results, whereas as a clear difference between QCD and QD was found only for the non-reactive surface configuration. This could indicate the difference in elastic scattering probabilities found is primarily caused by those surfaces that show a low reactivity, although further work would be required to fully investigate this finding.

Finally, we aimed at getting a better understanding of surface atom degrees of freedom that play a relevant role in describing the surface temperature effects with the SCM approach. Reaction and elastic scattering probabilities were obtained using EAM-SCM where only one, three, or five surface atoms were thermally displaced. These probabilities were then compared to those obtained using both the BOSS model and the full EAM-SCM. We found that including distortions of only one surface atom into the system was not sufficient to accurately describe the surface temperature effects of the system, with those results more closely resembling the BOSS results than the EAM-SCM results. Only when a total of five surface atom degrees of freedom were included in the model did we find close to an accurate description of the thermally distorted surface. A clear difference was already found between the elastic scattering probabilities obtained using QD and QCD even for those curves where only a single distorted surface was included in the EAM-SCM.

Previous work has already shown that the underlying DFT functional of V_{coup} is transferable between different facets of the copper surface,[40,57] which opens up the opportunity to expand this work further toward the Cu(100) facet and eventually the Cu(211) stepped surface. However, the number of surface slabs in the Monte Carlo sampling in this work was quite limited (104), and as such we expect to obtain more definitive results once more QD-EAM-SCM simulations can be performed, also including the results from different initial rovibrational states of H_2. Additional work is required to allow for accurate results of reactive scattering from surface slabs below ~300 K,[41] as the classical MD approach to generating slabs with the EAM is expected not to give accurate results, predominantly because the use of a thermostat that extracts the zero point energy from the Cu system, but also from implicitly employing a Maxwell–Boltzmann statistical sampling of the phonons that are actually bosons and adhere to the Bose–Einstein statistics.[8]

SUPPLEMENTARY MATERIAL

See the supplementary material for the computational details of the TDWP quantum dynamics simulations of H_2 dissociation on a Cu(111) surface.

ACKNOWLEDGMENTS

The authors thank Professor Dr. G. J. Kroes and NWO-EW for providing the computational resources needed to obtain these results and the rest of the theoretical chemistry group for their feedback on this project.

AUTHOR DECLARATIONS

Conflict of Interest

The authors have no conflicts to disclose.

DATA AVAILABILITY

The data that support the findings of this study are available from the research group's public repository at https://pubs.tc.lic.leidenuniv.nl/.

REFERENCES

[1] G. J. Kroes, and C. Díaz, "Quantum and classical dynamics of reactive scattering of H_2 from metal surfaces," Chem. Soc. Rev. **45**, 3658–3700 (2016).
[2] G. J. Kroes, "Computational approaches to dissociative chemisorption on metals: Towards chemical accuracy," Phys. Chem. Chem. Phys. **23**, 8962–9048 (2021).
[3] Y. Xiao, W. Dong, and H. F. Busnengo, "Reactive force fields for surface chemical reactions: A case study with hydrogen dissociation on Pd surfaces," J. Chem. Phys. **132**, 014704 (2010).
[4] A. Mondal, M. Wijzenbroek, M. Bonfanti, C. Díaz, and G. J. Kroes, "Thermal lattice expansion effect on reactive scattering of H_2 from Cu(111) at T_s = 925 K," J. Phys. Chem. A **117**, 8770–8781 (2013).
[5] G. N. Seminara, I. F. Peludhero, W. Dong, A. E. Martínez, and H. F. Busnengo, "Molecular dynamics study of molecular and dissociative adsorption using system-specific force fields based on ab initio calculations: CO/Cu(110) and CH_4/Pt(110)," Top. Catal. **62**, 1044–1052 (2019).
[6] A. K. Tiwari, S. Nave, and B. Jackson, "The temperature dependence of methane dissociation on Ni(111) and Pt(111): Mixed quantum-classical studies of the lattice response," J. Chem. Phys. **132**, 134702 (2010).
[7] H. Guo, A. Farjamnia, and B. Jackson, "Effects of lattice motion on dissociative chemisorption: Toward a rigorous comparison of theory with molecular beam experiments," J. Phys. Chem. Lett. **7**, 4576–4584 (2016).
[8] J. Dutta, S. Mandal, S. Adhikari, P. Spiering, J. Meyer, and M. F. Somers, "Effect of surface temperature on quantum dynamics of H_2 on Cu(111) using a chemically accurate potential energy surface," J. Chem. Phys. **154**, 104103 (2021).
[9] F. Nattino, C. Díaz, B. Jackson, and G. J. Kroes, "Effect of surface motion on the rotational quadrupole alignment parameter of D_2 reacting on Cu(111)," Phys. Rev. Lett. **108**, 236104 (2012).
[10] M. Wijzenbroek and M. F. Somers, "Static surface temperature effects on the dissociation of H_2 and D_2 on Cu(111)," J. Chem. Phys. **137**, 054703 (2012).
[11] P. Spiering, M. Wijzenbroek, and M. F. Somers, "An improved static corrugation model," J. Chem. Phys. **149**, 234702 (2018).
[12] B. Smits and M. F. Somers, "Beyond the static corrugation model: Dynamic surfaces with the embedded atom method," J. Chem. Phys. **154**, 074710 (2021).

[13]B. Jackson, "Quantum studies of methane-metal inelastic diffraction and trapping: The variation with molecular orientation and phonon coupling," Chem. Phys. **559**, 111516 (2022).
[14]C. Smith, A. K. Hill, and L. Torrente-Murciano, "Current and future role of Haber–Bosch ammonia in a carbon-free energy landscape," Energy Environ. Sci. **13**, 331–344 (2020).
[15]T. Zambelli, J. V. Barth, J. Wintterlin, and G. Ertl, "Complex pathways in dissociative adsorption of oxygen on platinum," Nature **390**, 495–497 (1997).
[16]H. F. Busnengo, A. Salin, and W. Dong, "Representation of the 6D potential energy surface for a diatomic molecule near a solid surface," J. Chem. Phys. **112**, 7641–7651 (2000).
[17]A. Lozano, X. J. Shen, R. Moiraghi, W. Dong, and H. F. Busnengo, "Cutting a chemical bond with demon's scissors: Mode- and bond-selective reactivity of methane on metal surfaces," Surf. Sci. **640**, 25–35 (2015).
[18]G. J. Kroes, M. Wijzenbroek, and J. R. Manson, "Possible effect of static surface disorder on diffractive scattering of H_2 from Ru(0001): Comparison between theory and experiment," J. Chem. Phys. **147**, 244705 (2017).
[19]N. Artrith and J. Behler, "High-dimensional neural network potentials for metal surfaces: A prototype study for copper," Phys. Rev. B **85**, 045439 (2012).
[20]L. Zhu, Y. Zhang, L. Zhang, X. Zhou, and B. Jiang, "Unified and transferable description of dynamics of H_2 dissociative adsorption on multiple copper surfaces *via* machine learning," Phys. Chem. Chem. Phys. **22**, 13958–13964 (2020).
[21]Q. Lin, L. Zhang, Y. Zhang, and B. Jiang, "Searching configurations in uncertainty space: Active learning of high-dimensional neural network reactive potentials," J. Chem. Theory Comput. **17**, 2691–2701 (2021).
[22]J. Behler, "First principles neural network potentials for reactive simulations of large molecular and condensed systems," Angew. Chem., Int. Ed. **56**, 12828–12840 (2017).
[23]M. F. Somers, R. A. Olsen, H. F. Busnengo, E. J. Baerends, and G. J. Kroes, "Reactive scattering of H_2 from Cu(100): Six-dimensional quantum dynamics results for reaction and scattering obtained with a new, accurately fitted potential-energy surface," J. Chem. Phys. **121**, 11379–11387 (2004).
[24]M. del Cueto, A. S. Muzas, M. F. Somers, G. J. Kroes, C. Díaz, and F. Martín, "Exploring surface landscapes with molecules: Rotationally induced diffraction of H_2 on LiF(001) under fast grazing incidence conditions," Phys. Chem. Chem. Phys. **19**, 16317–16322 (2017).
[25]A. S. Muzas, M. del Cueto, F. Gatti, M. F. Somers, G. J. Kroes, F. Martín, and C. Díaz, "H_2LiF(001) diffractive scattering under fast grazing incidence using a DFT-based potential energy surface," Phys. Rev. B **96**, 205432 (2017).
[26]C. Díaz, E. Pijper, R. A. Olsen, H. F. Busnengo, D. J. Auerbach, and G. J. Kroes, "Chemically accurate simulation of a prototypical surface reaction: H_2 dissociation on Cu(111)," Science **326**, 832–834 (2009).
[27]C. Díaz, R. A. Olsen, D. J. Auerbach, and G. J. Kroes, "Six-dimensional dynamics study of reactive and non reactive scattering of H_2 from Cu(111) using a chemically accurate potential energy surface," Phys. Chem. Chem. Phys. **12**, 6499–6519 (2010).
[28]F. Nattino, A. Genova, M. Guijt, A. S. Muzas, C. Díaz, D. J. Auerbach, and G. J. Kroes, "Dissociation and recombination of D_2 on Cu(111): *Ab initio* molecular dynamics calculations and improved analysis of desorption experiments," J. Chem. Phys. **141**, 124705 (2014).
[29]M. Bonfanti, M. F. Somers, C. Díaz, H. F. Busnengo, and G. J. Kroes, "7D quantum dynamics of H_2 scattering from Cu(111): The accuracy of the phonon sudden approximation," Z. Phys. Chem. **227**, 1397 (2013).
[30]G. J. Kroes, J. I. Juaristi, and M. Alducin, "Vibrational excitation of H_2 scattering from Cu(111): Effects of surface temperature and of allowing energy exchange with the surface," J. Phys. Chem. C **121**, 13617–13633 (2017).
[31]H. A. Michelsen, C. T. Rettner, D. J. Auerbach, and R. N. Zare, "Effect of rotation on the translational and vibrational energy dependence of the dissociative adsorption of D_2 on Cu(111)," J. Chem. Phys. **98**, 8294–8307 (1993).
[32]C. T. Rettner, H. A. Michelsen, and D. J. Auerbach, "Quantum-state-specific dynamics of the dissociative adsorption and associative desorption of H_2 at a Cu(111) surface," J. Chem. Phys. **102**, 4625–4641 (1995).
[33]H. Hou, S. J. Gulding, C. T. Rettner, A. M. Wodtke, and D. J. Auerbach, "The stereodynamics of a gas-surface reaction," Science **277**, 80–82 (1997).
[34]M. J. Murphy and A. Hodgson, "Adsorption and desorption dynamics of H_2 and D_2 on Cu(111): The role of surface temperature and evidence for corrugation of the dissociation barrier," J. Chem. Phys. **108**, 4199–4211 (1998).
[35]S. Kaufmann, Q. Shuai, D. J. Auerbach, D. Schwarzer, and A. M. Wodtke, "Associative desorption of hydrogen isotopologues from copper surfaces: Characterization of two reaction mechanisms," J. Chem. Phys. **148**, 194703 (2018).
[36]H. Chadwick, M. F. Somers, A. C. Stewart, Y. Alkoby, T. J. D. Carter, D. Butkovicova, and G. Alexandrowicz, "Stopping molecular rotation using coherent ultra-low-energy magnetic manipulations," Nat. Commun. **13**, 2287 (2022).
[37]O. Godsi, G. Corem, Y. Alkoby, J. T. Cantin, R. V. Krems, M. F. Somers, J. Meyer, G. J. Kroes, T. Maniv, and G. Alexandrowicz, "A general method for controlling and resolving rotational orientation of molecules in molecule-surface collisions," Nat. Commun. **8**, 15357 (2017).
[38]Y. Alkoby, H. Chadwick, O. Godsi, H. Labiad, M. Bergin, J. T. Cantin, I. Litvin, T. Maniv, and G. Alexandrowicz, "Setting benchmarks for modelling gas–surface interactions using coherent control of rotational orientation states," Nat. Commun. **11**, 3110 (2020).
[39]H. Chadwick, Y. Alkoby, J. T. Cantin, D. Lindebaum, O. Godsi, T. Maniv, and G. Alexandrowicz, "Molecular spin echoes; multiple magnetic coherences in molecule surface scattering experiments," Phys. Chem. Chem. Phys. **23**, 7673–7681 (2021).
[40]E. W. F. Smeets, G. Füchsel, and G. J. Kroes, "Quantum dynamics of dissociative chemisorption of H_2 on the stepped Cu(211) surface," J. Phys. Chem. C **123**, 23049–23063 (2019).
[41]H. W. Sheng, M. J. Kramer, A. Cadien, T. Fujita, and M. W. Chen, "Highly optimized embedded-atom-method potentials for fourteen fcc metals," Phys. Rev. B **83**, 134118 (2011).
[42]P. Spiering and J. Meyer, "Testing electronic friction models: Vibrational deexcitation in scattering of H_2 and D_2 from Cu(111)," J. Phys. Chem. Lett. **9**, 1803–1808 (2018).
[43]G. Füchsel, T. Klamroth, S. Monturet, and P. Saalfrank, "Dissipative dynamics within the electronic friction approach: The femtosecond laser desorption of H_2/D_2 from Ru(0001)," Phys. Chem. Chem. Phys. **13**, 8659 (2011).
[44]R. J. Maurer, B. Jiang, H. Guo, and J. C. Tully, "Mode specific electronic friction in dissociative chemisorption on metal surfaces: H_2 on Ag(111)," Phys. Rev. Lett. **118**, 256001 (2017).
[45]P. Spiering, K. Shakouri, J. Behler, G. J. Kroes, and J. Meyer, "Orbital-dependent electronic friction significantly affects the description of reactive scattering of N_2 from Ru(0001)," J. Phys. Chem. Lett. **10**, 2957–2962 (2019).
[46]V. F. Sears and S. A. Shelley, "Debye–Waller factor for elemental crystals," Acta Crystallogr., Sect. A: Found. Crystallogr. **47**, 441–446 (1991).
[47]M. Wijzenbroek and G. J. Kroes, "The effect of the exchange-correlation functional on H_2 dissociation on Ru(0001)," J. Chem. Phys. **140**, 084702 (2014).
[48]G. J. Kroes, and M. F. Somers, "Six-dimensional dynamics of dissociative chemisorption of H_2 on metal surfaces," J. Theor. Comput. Chem. **04**, 493–581 (2005).
[49]A. Vibok and G. G. Balint-Kurti, "Parametrization of complex absorbing potentials for time-dependent quantum dynamics," J. Phys. Chem. **96**, 8712–8719 (1992).
[50]G. G. Balint-Kurti, R. N. Dixon, and C. C. Marston, "Grid methods for solving the Schrödinger equation and time dependent quantum dynamics of molecular photofragmentation and reactive scattering processes," Int. Rev. Phys. Chem. **11**, 317–344 (1992).
[51]B. Jiang and H. Guo, "Six-dimensional quantum dynamics for dissociative chemisorption of H_2 and D_2 on Ag(111) on a permutation invariant potential energy surface," Phys. Chem. Chem. Phys. **16**, 24704–24715 (2014).
[52]G. J. Kroes, "Six-dimensional quantum dynamics of dissociative chemisorption of H_2 on metal surfaces," Prog. Surf. Sci. **60**, 1–85 (1999).

[53]C. C. Marston and G. G. Balint-Kurti, "The Fourier grid Hamiltonian method for bound state eigenvalues and eigenfunctions," J. Chem. Phys. **91**, 3571–3576 (1989).
[54]R. Bulirsch and J. Stoer, "Numerical treatment of ordinary differential equations by extrapolation methods," Numer. Math. **8**, 1–13 (1966).
[55]H. F. Busnengo, M. A. Di Césare, W. Dong, and A. Salin, "Surface temperature effects in dynamic trapping mediated adsorption of light molecules on metal surfaces: H_2 on Pd(111) and Pd(110)," Phys. Rev. B **72**, 125411 (2005).
[56]*Dynamics of Gas-Surface Interactions: Atomic-Level Understanding of Scattering Processes at Surfaces*, edited by R. D. Muino and H. F. Busnengo, Springer Series in Surface Sciences (Springer-Verlag, Berlin, Heidelberg, 2013).
[57]L. Sementa, M. Wijzenbroek, B. J. van Kolck, M. F. Somers, A. Al-Halabi, H. F. Busnengo, R. A. Olsen, G. J. Kroes, M. Rutkowski, C. Thewes, N. F. Kleimeier, and H. Zacharias, "Reactive scattering of H_2 from Cu(100): Comparison of dynamics calculations based on the specific reaction parameter approach to density functional theory with experiment," J. Chem. Phys. **138**, 044708 (2013).